AIP | Applied Physics Letters

Phase-field simulation of domain structures and magnetostrictive response in Tb1−xDyxFe2 alloys near morphotropic phase boundary

Cheng-Chao Hu, Tian-Nan Yang, Hou-Bing Huang, Jia-Mian Hu, Jian-Jun Wang, Yang-Guang Shi, Da-Ning Shi, and Long-Qing Chen

Citation: Applied Physics Letters **108**, 141908 (2016); doi: 10.1063/1.4945684
View online: http://dx.doi.org/10.1063/1.4945684
View Table of Contents: http://scitation.aip.org/content/aip/journal/apl/108/14?ver=pdfcov
Published by the AIP Publishing

Articles you may be interested in

Local rhombohedral symmetry in Tb0.3Dy0.7Fe2 near the morphotropic phase boundary
Appl. Phys. Lett. **105**, 192407 (2014); 10.1063/1.4901646

Domain rotation simulation of anisotropic magnetostrictions in giant magnetostrictive materials
J. Appl. Phys. **110**, 063901 (2011); 10.1063/1.3634115

Ferroelastic properties of oriented Tb x Dy 1−x Fe 2 polycrystals
Appl. Phys. Lett. **83**, 3960 (2003); 10.1063/1.1625427

Low field anisotropic magnetostriction of single domain exchange-coupled (TbFe/Fe) multilayers
J. Appl. Phys. **87**, 5783 (2000); 10.1063/1.372521

Magnetostrictive and magnetic properties of the pseudobinary compounds Pr x Tb 1−x Fe 2 and Pr 0.15 Tb x Dy 0.85−x Fe 2
J. Appl. Phys. **83**, 7753 (1998); 10.1063/1.367949

Reuse of AIP Publishing content is subject to the terms at: https://publishing.aip.org/authors/rights-and-permissions. Download to IP: 128.118.37.128 On: Mon, 16 May 2016 20:34:47

Phase-field simulation of domain structures and magnetostrictive response in $Tb_{1-x}Dy_xFe_2$ alloys near morphotropic phase boundary

Cheng-Chao Hu,[1,2] Tian-Nan Yang,[2] Hou-Bing Huang,[2,3] Jia-Mian Hu,[2] Jian-Jun Wang,[2,a)] Yang-Guang Shi,[1,b)] Da-Ning Shi,[1] and Long-Qing Chen[2]
[1]*Department of Applied Physics, Nanjing University of Aeronautics and Astronautics, Nanjing 210016, China*
[2]*Department of Materials Science and Engineering, The Pennsylvania State University, University Park, Pennsylvania 16802, USA*
[3]*Department of Physics, University of Science and Technology Beijing, Beijing 100083, China*

(Received 28 December 2015; accepted 27 March 2016; published online 6 April 2016)

Phase-field method micromagnetic microelastic modeling is employed to simulate the thermal domain stability and enhanced magnetostrictive responses around the ferromagnetic morphotropic phase boundary (MPB) in giant magnetostrictive $Tb_{1-x}Dy_xFe_2$ ($x \approx 0.27$) single crystal. The simulation shows that the rhombohedral and tetragonal phases coexist in equilibrium in the vicinity of MPB region due to the balance of weak magnetocrystalline anisotropy and strong exchange, magnetostatic and ferroelastic interaction. Enhanced magnetostrictive response is found in the vicinity of MPB, which could be attributed to the low-energy rotating pathways of local magnetization vectors in the phase coexisting region. © *2016 AIP Publishing LLC*.
[http://dx.doi.org/10.1063/1.4945684]

Morphotropic phase boundary (MPB) generally refers to a special transition region in the ferroelectric composition-temperature phase diagram, where two ferroelectric phases with different crystallographic symmetries are abruptly separated.[1–3] Near the MPB region, the free energy landscape is flat, allowing the polarization to rotate easily under a voltage and thus giving rise to an enhanced electromechanical response. Although most of the studies on MPB effects focused on ferroelectric systems, such as PZT ($PbZrO_3$-$PbTiO_3$),[4] PMN-PT ($PbMg_{1/3}Nb_{2/3}O_3$-$PbTiO_3$),[5] and BZT-BCT ($Ba(Zr_{0.2}Ti_{0.8})O_3$-$(Ba_{0.7}Ca_{0.3})O_3$),[6] it has been proposed that MPB might be a universal effect in both ferroelectric and ferromagnetic systems.[7,8]

Giant magnetostrictive materials, as modern smart materials, are playing an increasingly more important role in many applications, such as ultra-sensitive sensors, high energy density actuators, acoustic transducers, etc.[9] In the past decades, in order to exploit the giant magnetostriction at low field, much effort has been devoted to seek an anisotropy compensation system. Recently, Yang *et al*. experimentally found that the boundary separating the easy magnetic directions (EMD) $M_s \parallel [111]$ and $M_s \parallel [100]$ indeed corresponds to the boundary separating the rhombohedral (R) and tetragonal (T) structures, and the anisotropy compensation area is analogous to a ferroelectric MPB.[10] Bergstrom *et al*. reported a ferromagnetic MPB in $Tb_{1-x}Dy_xFe_2$ (Terfenol-D) and found that the traditional single-ion model could not account for the temperature dependence for the transition width near the MPB.[11] Zhou *et al*. reported a ferromagnetic MPB in $Tb_{1-x}Gd_xCo_2$ system, showing another type of MPB wherein giant susceptibility with zero strain was observed.[12] Ma *et al*. found a coexistence of R and T phases over a wide range of temperatures and observed nanodomain microstructures in $Tb_{0.3}Dy_{0.7}Fe_2$.[13] Adil *et al*. also found a coexistence of R and T phases near the MPB of $Tb_{1-x}Gd_xFe_2$ system by synchrotron x-ray diffraction.[14] Earlier Mössbauer-effect studies on $Tb_{1-x}Ho_xFe_2$ system showed a magnetic order "*triple phase point*" behavior.[15] All these systems together show the rising interest in ferromagnetic MPB, which might greatly enrich the connotation and extension of MPB. Moreover, because of the optimized magnetostrictive property and susceptibility in the vicinity of MPB, the mechanism of phase transition and the detailed domain microstructure is a question of both scientific and technological importance.

In spite of such wide experimental studies in ferromagnetic MPB, the insight of the domain structures and switching near ferromagnetic MPB is still lacking. Several phenomenological approximations have been developed to explain the magnetostrictive behavior of Terfenol-D with composition near $Tb_{0.27}Dy_{0.73}Fe_2$.[16–21] Mechanisms proposed so far, however, mostly focus on the evolution of domains of rhombohedral phase and assume that each domain evolves independently and is not affected by neighboring domains, which means no strain compatibility and intrinsic stress were considered. As a matter of fact, in real materials, multi-phases domain structures are expected because of the low magnetocrystalline anisotropy and nanoscale decomposition microstructures in the vicinity of MPB area.[13] Moreover, the intrinsic stress caused by the elastic incompatibility is critically important, especially in materials with large intrinsic strain such as giant magnetostrictive materials. The phase-field method, which incorporates the micromagnetic and microelastic theories, has been demonstrated to be a powerful tool for studying the domain structures in magnetostrictive materials.[22–25] In this work, in order to consider the effects from the multi-phase coexistence and elastic incompatibility

a)Electronic mail: jzw12@psu.edu
b)Electronic mail: shiyangguang@gmail.com

 © 2016 AIP Publishing LLC

Reuse of AIP Publishing content is subject to the terms at: https://publishing.aip.org/authors/rights-and-permissions. Download to IP: 128.118.37.128 On: Mon, 16 May 2016 20:34:47

near MPB, we employ the phase-field method to study the temperature dependence of domain structures and switching in $Tb_{1-x}Dy_xFe_2$ ($x \approx 0.27$) single crystal.

In the phase-field model of ferromagnetics, the magnetic domain microstructure is described by the spatial distribution of the local magnetization $\boldsymbol{M}(m_1,m_2,m_3)$, where m_i are the components of unite magnetization vector, $\boldsymbol{m} = \boldsymbol{M_i}/M_s$. The equilibrium and transient magnetization configuration is evolved by the Landau-Lifshitz-Gilbert (LLG) equation, which is described as

$$(1+\alpha^2)\frac{\partial \mathbf{M}}{\partial t} = -\gamma_0 \mathbf{M} \times \mathbf{H}_{eff} - \frac{\gamma_0 \alpha}{M_s}\mathbf{M} \times (\mathbf{M} \times \mathbf{H}_{eff}), \quad (1)$$

where M_s the saturation magnetization, α and γ_0 the damping constant and the gyromagnetic ratio, respectively. $\boldsymbol{H}_{eff}$ is the effective magnetic field, determined by $\mathbf{H}_{eff} = -(\mu_0 M_s)^{-1}(\delta E_{tot}/\delta \boldsymbol{m})$ with μ_0 the vacuum permeability and E_{tot} the total free energy. The E_{tot} is written as

$$E_{tot} = E_{ani} + E_{ms} + E_{exc} + E_{el} + E_{ext}, \quad (2)$$

where E_{ani}, E_{ms}, E_{exc}, E_{el}, and E_{ext} are the magnetocrystalline anisotropy, magnetic exchange, magnetostatic, elastic, and external energies, respectively. The magnetocrystalline anisotropy energy can be written as

$$E_{ani} = \int\int\int_V [K_1(m_1^2m_2^2 + m_2^2m_3^2 + m_3^2m_1^2) + K_2 m_1^2 m_2^2 m_3^2]dV, \quad (3)$$

where K_1 and K_2 the magnetocrystalline anisotropy coefficients, and V is the total volume of the system. The elastic energy generated from the local deformation can be expressed as

$$E_{el} = \int\int\int_V \frac{1}{2}c_{ijkl}e_{ij}e_{kl}dV = \int_V \frac{1}{2}c_{ijkl}\left(\varepsilon_{ij} - \varepsilon_{ij}^0\right)\left(\varepsilon_{kl} - \varepsilon_{kl}^0\right)dV, \quad (4)$$

where c_{ijkl} the elastic stiffness tensor, e_{ij} the elastic strain, ε_{ij} the total strain, and ε_{ij}^0 the stress-free strain. In cubic magnetostrictive materials, the stress-free strain ε_{ij}^0 denotes the spontaneous lattice deformation coupled to the local magnetization and is given by

$$\varepsilon_{ij}^0 = \begin{cases} \frac{3}{2}\lambda_{100}\left(m_i m_j - \frac{1}{3}\right) & (i=j) \\ \frac{3}{2}\lambda_{111} m_i m_j & (i \neq j), \end{cases} \quad (5)$$

where λ_{100} and λ_{111} the magnetostrictive constants. According to Khachaturyan's mesoscopic elastic theory,[26] the total strain ε_{ij} can be represented as the sum of homogeneous strain $\bar{\varepsilon}$ and heterogeneous strain ε_{ij}^{het}, i.e., $\varepsilon_{ij} = \bar{\varepsilon} + \varepsilon_{ij}^{het}$.

The heterogeneous strain follows the integral relationship of $\int\int\int_V \varepsilon_{ij}^{het} dV = 0$ and can be further described using the displacement $u_i(\mathbf{r})$ as

$$\varepsilon_{ij}^{het} = \frac{1}{2}\left(\frac{\partial u_i}{\partial x_j} + \frac{\partial u_j}{\partial x_i}\right). \quad (6)$$

The $u_i(\mathbf{r})$ can be solved using Khachaturyan's microelasticity theory.[26] The formulation of other energy terms of E_{ms}, E_{exc}, and E_{ext} could be found in Ref. 22. The evolution of domain microstructure is described by the LLG equation, which is numerically solved using the Gauss-Seidel projection method.[27]

In the simulation, a model size of $512\Delta x \times 512\Delta x \times 1\Delta x$ with cell size Δx of 5 nm, and periodic boundary condition are employed. The initial domain structure is created by assigning random orientations for the magnetization configuration. The corresponding material parameters are obtained from previous experiments and theoretical calculation.[9,16,28–30] Similar as how Atzmony[15] and Bergstrom[11] did, due to the lack of some experimental data, here we assume $K_i(Tb_{1-x}Dy_xFe_2) = (1-x)K_i(TbFe_2) + xK_i(DyFe_2)$, where K_i are the ith order magnetocrystalline anisotropy coefficients at different temperatures.[31] The K_i of parent alloys $TbFe_2$ and $DyFe_2$ at different temperatures have been calculated in Ref. 29.

The change in domain structure of $Tb_{0.27}Dy_{0.73}Fe_2$ with temperature as shown in Fig. 1 indicates a bridging domain mechanism for phase coexistence around MPB.

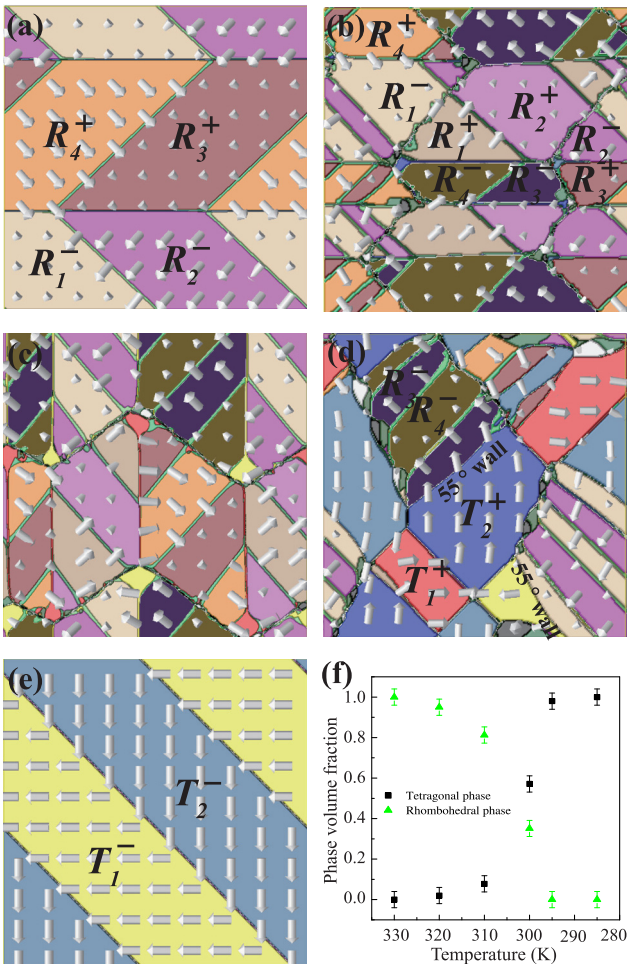

FIG. 1. Magnetization domain structures (arrows show different magnetization direction) of $Tb_{0.27}Dy_{0.73}Fe_2$: R_1^+: (1, 1, 1); R_1^-: (−1, −1, −1); R_2^+: (1, 1, −1); R_2^-: (−1, −1, 1); R_3^+: (1, −1, −1); R_3^-: (−1, 1, 1); R_4^+: (1, −1, 1); R_4^-: (−1, 1, −1) and T_1^+: (1, 0, 0); T_1^-: (−1, 0, 0); T_2^+: (0, 1, 0); T_2^-: (0, −1, 0); T_3^+: (0, 0, 1); T_3^-: (0, 0, −1) at (a) $T = 330$ K; (b) $T = 320$ K; (c) $T = 310$ K; (d) $T = 300$ K; (e) $T = 280$ K; and (f) corresponding phase volume fraction under different temperatures.

Reuse of AIP Publishing content is subject to the terms at: https://publishing.aip.org/authors/rights-and-permissions. Download to IP: 128.118.37.128 On: Mon, 16 May 2016 20:34:47

From Figs. 1(a) and 1(e), it can be seen that when the temperature is away from the MPB area, domains of tetragonal phase mutually form twins of {110} boundaries with 90° domain walls, while domains of rhombohedral phase form twins of either {110} or {100} boundaries with 71° and 109° domain walls. These simulation results are in agreement with the crystallographic analysis of domain microstructure and previous experimental results.[32–37] At 310 K (Fig. 1(c)), the minority tetragonal phase spontaneously coexists with and bridges the domains of the majority rhombohedral phase in different orientated domain boundaries. As shown in Figs. 2(b) and 2(c), this existence of minor tetragonal phase as bridging domains increases the anisotropy energy but effectively reduces other energies including the magnetic exchange energy, magnetostatic energy, and elastic energy, leading to the decrease in total energy. The local energy minimum as well as the inhomogeneous internal stress distribution among the domain boundaries with multiple structure variants together provides a favorable configuration and natural mechanism for phase coexistence. In fact, a very recent high resolution transmission electron microscopy experiment has provided the direct evidence for the nanoscale tetragonal domains coexisting with the local strip-like rhombohedral domain,[13] which is similar with our simulation results.

The more interesting result is that complex poly-domain microstructure with mixed rhombohedral and tetragonal phases appears near the center area of MPB at 300 K, as shown in Fig. 1(d). This spontaneously formed multi-phase domain structure has not been observed before probably because existing efforts were mainly focused on the rhombohedral side of MPB. It is worth noting that under the condition of low magnetocrystalline anisotropy as shown in Fig. 2(a), the energy gap between rhombohedral and tetragonal phase are drastically reduced, leading to a weakness of the coupling between magnetization and atomic framework. Consequently, domain morphologies will be strongly influenced by the long-range elastic interactions arising from the accommodation of misfit strain and elastic inhomogeneity among multiple structure orientation variants.[38] Energy analysis (Fig. 2(f)) indicates that the R-T 55° domain wall has the lowest total energy density compared with the R-R and T-T domain walls, which further stabilizes the phase coexistence. The lower R-T 55° domain wall energy is the result of the lower anisotropy, exchange, magnetostatic energy density, as well as the releasing elastic energy density to achieving domain-average stress accommodation.[39] Phase volume fraction analysis (Fig. 1(f)) shows that the temperature range for the existence of a multi-phase poly-domain is about 25 K (from 295 K to 320 K), wherein rhombohedral and tetragonal phases coexist. In particular, as will be shown in the following, this configuration of coherent domain microstructure could provide a low-energy pathway for magnetization transition between different magnetic easy axes.

The simulated strains of $Tb_{0.27}Dy_{0.73}Fe_2$ at various temperatures are shown in Fig. 3(a). As expected, the strain at 285 K is low because of the small λ_{100}. While for the case in the vicinity of MPB with temperature range from 300 K to 320 K, the widely observed dramatic increases in experiments[40–42] are obtained. Domain microstructure evolution analysis shows that the large increase is due to both the magnetization rotation and associated domain wall motion, which is consistent with previous simulation results on growth twinned Terfenol-D.[23] It is worth noting that the lowest critical field H_{cr} appears at 300 K, while it increases with the temperature away from MPB. The detailed domain evolution with increasing applied fields corresponding to A, B, and C in Fig. 3(a) are shown in Figs. 3(b), 3(c), and 3(d). Fig. 3(e) is used to schematically show the domain evolution: the rhombohedral phase domains which are away from the direction of the applied field, such as R_3^- and R_4^-, gradually disappear while the tetragonal domain T_2^+ increases due to the domain wall motion; thereafter, rhombohedral phase domains which are near the applied field, such as R_1^+ and R_2^+, appear near the boundary of T_1^+ domain and T_2^+ domain by the domain switching, which means, tetragonal phase as an intermediate phase provides a low-energy pathway for the rhombohedral phase domains rotation from the direction away from the applied field to that near the applied field.

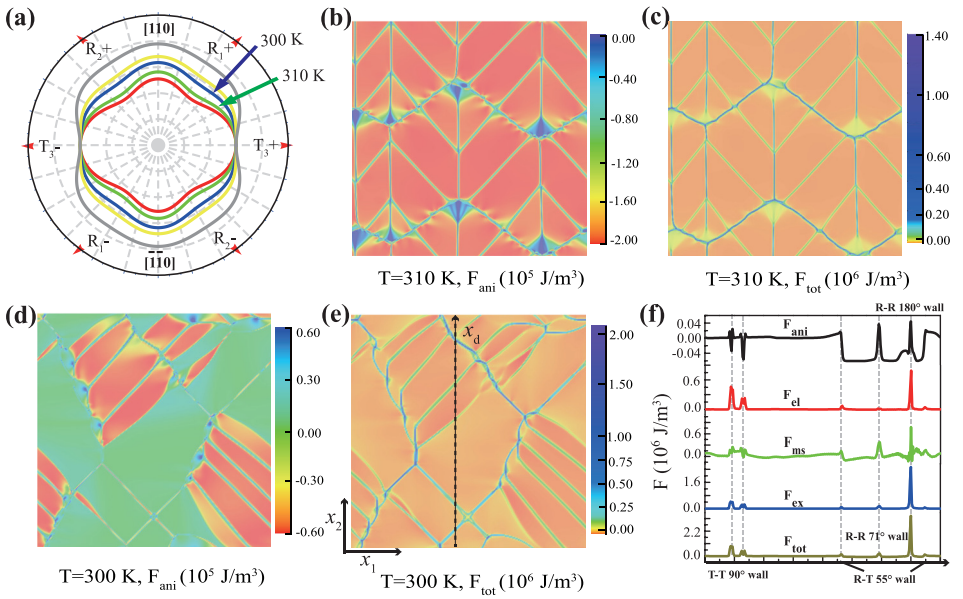

FIG. 2. (a) Thermodynamic analysis of anisotropy energy profile within ($\bar{1}$10) plane at different temperatures for $Tb_{0.27}Dy_{0.73}Fe_2$. Distribution of (b) magnetocrystalline anisotropy energy density and (c) total energy density corresponding to the domain structure in Fig. 1(c). Distribution of (d) magnetocrystalline anisotropy energy density and (e) total energy density corresponding to the domain structure in Fig. 1(d). (f) Anisotropy, elastic, magnetostatic, exchange, and total energy density distributions along the marked line of x_d in (e).

Reuse of AIP Publishing content is subject to the terms at: https://publishing.aip.org/authors/rights-and-permissions. Download to IP: 128.118.37.128 On: Mon, 16 May 2016 20:34:47

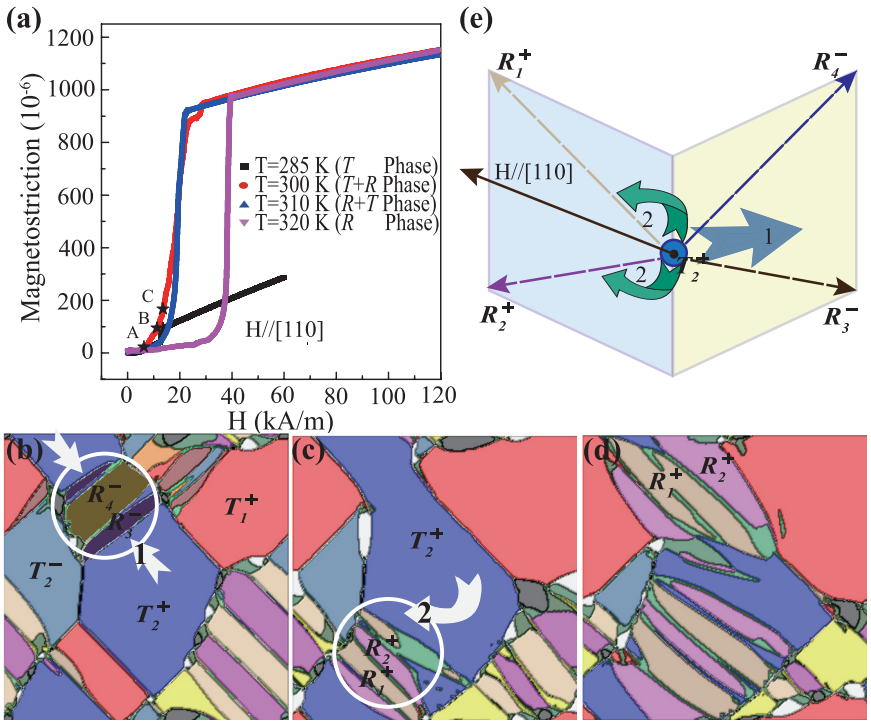

FIG. 3. (a) Magnetostriction of $Tb_{0.27}Dy_{0.73}Fe_2$ at various temperatures of $T = 285$ K, 300 K, 310 K, and 320 K. (b)–(d) Typical domain structures evolution corresponding to A, B, and C in (a) (the circle 1 and straight arrow show the domain wall motion from T_2^+ to R_3^- and R_4^- domains, circle 2 and curved arrow show the domain switching from T_2^+ to R_1^+ and R_2^+ domains). (e) Schematic overview of domain wall motion and domain switching as shown in (b)–(d).

This low-energy intermediate state together with the multifaceted rhombohedral phase domains provides the large strain response at low field.

In conclusion, the temperature dependence of domain microstructures and strain behaviors of $Tb_{0.27}Dy_{0.73}Fe_2$ (Terfenol-D) are systematically simulated by using a phase-field micromagnetic microelastic method. A bridging domain mechanism is proposed to account for the predicated phase coexistence. The tetragonal phase, as an intermediate, provides a low-energy pathway for the rotation of the rhombohedral phase domains from other directions to the direction of the external field, which explains the enhanced magnetostrictive response around MPB. Similar bridging domain mechanism was also proposed in ferroelectric PZT system,[43] which indicates the domain-level physical parallelism between ferromagnetic and ferroelectric MPB. It could be understandable by the similar characteristic energy terms described in ferromagnetic and ferroelectric systems: magnetocrystalline anisotropy energy–bulk chemical energy, exchange energy–gradient energy, magnetoelastic energy–electroelastic energy, and magnetoststic energy–electrostatic energy. The difference between ferroelectric MPB and ferromagnetic MPB mainly comes from the different behavior of polarization and spin. As for detailed difference between effects from different energy contributions to the stability of MPB in ferroelectrics and ferromagnetics, a systematical simulation need to be performed for making comparison. Finally, it is noteworthy that this phase-field modeling could also be used to predict the composition dependence of domain structures if the related material parameters are available. The present work intuitively elaborates the microscopic mechanism for the domain-strain behavior near a ferromagnetic MPB and is expected to stimulate future experimental, theoretical and engineering efforts on developing devices based on the unique behavior in ferromagnetic MPB.

This work was supported by the NSF under Grant No. DMR 1410714, NSF of China (Grant Nos. 11475086, 11374159, and 11504020), the Funding of Jiangsu Innovation Program for Graduate Education (Grant No. CXLX13_128), and the Funding for Outstanding Doctoral Dissertation in NUAA (Grant No. BCXJ13-16). C. C. Hu was sponsored by the China Scholarship Council. The computer simulations were carried out on the LION clusters at the Pennsylvania State University.

[1]B. Jaffe, W. R. Cook, and H. Jaffe, *Piezoelectric Ceramics* (Academic Press, New York, 1971).
[2]K. Uchino, *Ferroelectric Devices* (Marcel Dekker, New York, 2000).
[3]M. Ahart, M. Somayazulu, R. E. Cohen, P. Ganesh, P. Dera, H. K. Mao, R. J. Hemley, Y. Ren, P. Liermann, and Z. G. Wu, Nature (London) **451**, 545 (2008).
[4]B. Jaffe, R. S. Roth, and S. Marzullo, J. Appl. Phys. **25**, 809 (1954).
[5]S. E. Park and T. R. Shrout, J. Appl. Phys. **82**, 1804 (1997).
[6]W. F. Liu and X. B. Ren, Phys. Rev. Lett. **103**, 257602 (2009).
[7]R. E. Newnham, Acta Crystallogr., Sect. A **54**, 729 (1998).
[8]J. G. A. Rossetti, A. G. Khachaturyan, G. Akcay, and Y. Ni, J. Appl. Phys. **103**, 114113 (2008).
[9]A. E. Clark, in *Ferromagnetic Materials*, edited by E. P. Wohlfarth (North-Holland, Amsterdam, 1980), Vol. 1, p. 531.
[10]S. Yang, H. Bao, C. Zhou, Y. Wang, X. Ren, Y. Matsushita, Y. Katsuya, M. Tanaka, K. Kobayashi, X. Song *et al.*, Phys. Rev. Lett. **104**, 197201 (2010).
[11]R. Bergstrom, Jr., M. Wuttig, J. Cullen, P. Zavalij, R. Briber, C. Dennis, V. O. Garlea, and M. Laver, Phys. Rev. Lett. **111**, 017203 (2013).
[12]C. Zhou, S. Ren, H. Bao, S. Yang, Y. Yao, Y. Ji, X. Ren, Y. Matsushita, Y. Katsuya, M. Tanaka *et al.*, Phys. Rev. B **89**, 100101(R) (2014).
[13]T. Y. Ma, X. L. Liu, X. W. Pan, X. Li, Y. Z. Jiang, M. Yan, H. Y. Li, M. X. Fang, and X. B. Ren, Appl. Phys. Lett. **105**, 192407 (2014).
[14]M. Adil, S. Yang, M. Mi, C. Zhou, J. Q. Wang, R. Zhang, X. Q. Liao, Y. Wang, X. B. Ren, X. P. Song, and Y. Ren, Appl. Phys. Lett. **106**, 132403 (2015).
[15]U. Atzmony, M. P. Dariel, E. R. Bauminger, D. Lebenbaum, I. Nowik, and S. Ofer, Phys. Rev. Lett. **28**, 244 (1972).
[16]A. E. Clark, H. T. Savage, and M. L. Spano, IEEE Trans. Magn. **20**, 1443 (1984).
[17]D. C. Jiles and J. B. Thoelke, J. Magn. Magn. Mater. **134**, 143 (1994).

Reuse of AIP Publishing content is subject to the terms at: https://publishing.aip.org/authors/rights-and-permissions. Download to IP: 128.118.37.128 On: Mon, 16 May 2016 20:34:47

[18]A. DeSimone and R. D. James, J. Appl. Phys. **81**, 5706 (1997).
[19]X. G. Zhao and D. G. Lord, J. Magn. Magn. Mater. **195**, 699 (1999).
[20]W. D. Armstrong, J. Magn. Magn. Mater. **263**, 208 (2003).
[21]C. C. Hu, Y. G. Shi, D. N. Shi, S. L. Tang, J. Y. Fan, and Y. W. Du, J. Appl. Phys. **113**, 203906 (2013).
[22]J. X. Zhang and L. Q. Chen, Acta Mater. **53**, 2845 (2005).
[23]Y. Y. Huang and Y. M. Jin, Appl. Phys. Lett. **93**, 142504 (2008).
[24]P. P. Wu, X. Q. Ma, J. X. Zhang, and L. Q. Chen, J. Appl. Phys. **104**, 073906 (2008).
[25]H. B. Huang, X. Q. Ma, J. J. Wang, Z. H. Liu, W. Q. He, and L. Q. Chen, Acta Mater. **83**, 333 (2015).
[26]A. G. Khachaturyan, *Theory of Structural Transformation in Solids* (Wiley, New York, 1983).
[27]X. P. Wang, C. J. García-Cervera, and E. Weinan, J. Comput. Phys. **171**, 357 (2001).
[28]B. L. Wang and Y. M. Jin, J. Appl. Phys. **111**, 103908 (2012).
[29]K. N. Martin, P. A. J. de Groot, B. D. Rainford, K. Wang, G. J. Bowden, J. P. Zimmermann, and H. Fangohr, J. Phys. Condens. Matter **18**, 459 (2006).
[30]Y. C. Shu, M. P. Lin, and K. C. Wu, Mech. Mater. **36**, 975 (2004).
[31]$T = 285$ K: $K_1 = 1.2 \times 10^5$ J/m^3, $K_2 = -4.9 \times 10^5$ J/m^3; $T = 295$ K: $K_1 = 0.55 \times 10^5$ J/m^3, $K_2 = -4.1 \times 10^5$ J/m^3; $T = 300$ K: $K_1 = 0.24 \times 10^5$ J/m^3, $K_2 = -3.8 \times 10^5$ J/m^3; $T = 310$ K: $K_1 = -0.24 \times 10^5$ J/m^3, $K_2 = -3.2 \times 10^5$ J/m^3; $T = 320$ K: $K_1 = -0.6 \times 10^5$ J/m^3, $K_2 = -2 \times 10^5$ J/m^3; $T = 330$ K: $K_1 = -0.8 \times 10^5$ J/m^3, $K_2 = -1.6 \times 10^5$ J/m^3; $M_s = 8 \times 10^5$ A/m, $\lambda_{111} = 1600$ ppm, $\lambda_{100} = 100$ ppm, $c_{11} = 1.41 \times 10^{11}$ N/m^{11}, $c_{12} = 6.48 \times 10^{10}$ N/m^{11}, $c_{44} = 4.87 \times 10^{10}$ N/m^{11}, $A = 9 \times 10^{-12}$ J/m, $\alpha = 0.1$, $\gamma_0 = 2.21 \times 10^5$ m/A/s (Refs. 9, 16, and 28–30).
[32]G. H. Wu, X. G. Zhao, J. H. Wang, J. Y. Li, K. C. Jia, and W. S. Zhan, Appl. Phys. Lett. **67**, 2005 (1995).
[33]R. S. Sery, H. T. Savage, B. K. Tanner, and G. F. Clark, J. Appl. Phys. **49**, 2010 (1978).
[34]A. P. Holden, D. G. Lord, and P. J. Grundy, J. Appl. Phys. **79**, 4650 (1996).
[35]D. G. Lord, A. P. Holden, and P. J. Grundy, J. Appl. Phys. **81**, 5728 (1997).
[36]J. Dooley, M. D. Graef, and M. E. McHenry, J. Appl. Phys. **83**, 6837 (1998).
[37]G. F. Clark, B. K. Tanner, and H. T. Savage, Philos. Mag. B **46**, 331 (1982).
[38]A. G. Khachaturyan, Philos. Mag. **90**, 37 (2010).
[39]D. D. Viehland and E. K. H. Salje, Adv. Phys. **63**(4), 267 (2014).
[40]A. E. Clark, J. P. Teter, and O. D. McMasters, J. Appl. Phys. **63**, 3910 (1988).
[41]N. Galloway, M. P. Schulze, R. D. Greenough, and D. C. Jiles, Appl. Phys. Lett. **63**, 842 (1993).
[42]Y. Zhao, C. B. Jiang, H. Zhang, and H. B. Xu, J. Alloys Compd. **354**, 263 (2003).
[43]W. F. Rao and Y. U. Wang, Appl. Phys. Lett. **90**, 182906 (2007).

Reuse of AIP Publishing content is subject to the terms at: https://publishing.aip.org/authors/rights-and-permissions. Download to IP: 128.118.37.128 On: Mon, 16 May 2016 20:34:47